Magnetohydrodynamics, charged currents and directed flow in heavy ion collisions

Umut Gürsoy[1], Dmitri Kharzeev[2,3] and Krishna Rajagopal[4]

[1] *Institute for Theoretical Physics, Utrecht University*
Leuvenlaan 4, 3584 CE Utrecht, The Netherlands

[2] *Department of Physics and Astronomy, Stony Brook University, New York 11794, USA*

[3] *Department of Physics, Brookhaven National Laboratory, Upton, New York 11973, USA and*

[4] *Center for Theoretical Physics, Massachusetts Institute of Technology, Cambridge, MA 02139.*
(Dated: January 17, 2014)

The hot QCD matter produced in any heavy ion collision with a nonzero impact parameter is produced within a strong magnetic field. We study the imprint that these fields leave on the azimuthal distributions and correlations of the produced charged hadrons. The magnetic field is time-dependent and the medium is expanding, which leads to the induction of charged currents due to the combination of Faraday and Hall effects. We find that these currents result in a charge-dependent directed flow v_1 that is odd in rapidity and odd under charge exchange. It can be detected by measuring correlations between the directed flow of charged hadrons at different rapidities, $\langle v_1^\pm(y_1) v_1^\pm(y_2) \rangle$.

PACS numbers:

I. INTRODUCTION

Strong magnetic fields $\vec{B}$ are produced in all non-central heavy ion collisions (i.e. those with nonzero impact parameter b) by the charged "spectators" (i.e. the nucleons from the incident nuclei that "miss", flying past each other rather than colliding). Indeed, estimates obtained via application of the Biot-Savart law to heavy ion collisions with $b = 4$ fm yield $e|\vec{B}|/m_\pi^2 \approx$ 1-3 about 0.1-0.2 fm/c after a RHIC collision with $\sqrt{s} = 200$ AGeV and $e|\vec{B}|/m_\pi^2 \approx$ 10-15 at some even earlier time after an LHC collision with $\sqrt{s} = 2.76$ ATeV [1–7]. In recent years there has been much interest in consequences of these enormous magnetic fields present early in the collision that are observable in the final state hadrons produced by the collision. In particular, the interplay of magnetic field and quantum anomalies has been predicted to lead to a number of interesting phenomena, including the chiral magnetic effect [1, 8], a quadrupole deformation of the electric charge distribution induced by a chiral magnetic wave [9, 10], and the enhanced anisotropic production of soft photons through "magneto-sonoluminescence" – the conversion of phonons into photons in an external magnetic field [11]. While several of the predicted effects have been observed in heavy ion collision data [12–18], it is often hard to distinguish them unambiguously from a combination of mundane phenomena possibly present in the anisotropic expansion of quark-gluon matter, see e.g. Refs. [19–21]. This makes it imperative to establish that the presence of an early-time magnetic field can have observable consequences on the motion of the final-state charged particles seen in detectors, making it possible to use data to calibrate the strength of the magnetic field.

In this paper we analyze what are surely the simplest and most direct effects of magnetic fields in heavy ion collisions, and quite likely also their largest effects, namely the induction of electric currents carried by the charged quarks and antiquarks in the quark-gluon plasma (QGP) and, later, by the charged hadrons. The source of these charged currents is twofold. Firstly, the magnitude of $\vec{B}$ varies in time, decreasing as the charged spectators fly away along the beam direction, receding from the QGP produced in the collision. The changing $\vec{B}$ results in an electric field due to Faraday's law, and this in turn produces an electric current in the conducting medium. Secondly, because the conducting medium, i.e. the QGP, has a significant initial longitudinal expansion velocity $\vec{u}$ parallel to the beam direction and therefore perpendicular to $\vec{B}$, the Lorentz force results in an electric current perpendicular to both the velocity and $\vec{B}$, akin to the classical Hall effect. (We shall refer to this current as a Hall current throughout, even though this nomenclature may not be quite right since our system has no edge at which charges can build up.) Fig. 1 serves to orient the reader as to the directions of $\vec{B}$ and $\vec{u}$, and the electric currents induced by the Faraday and Hall effects. The net electric current is the sum of that due to Faraday and that due to Hall. If the Faraday effect is stronger than the Hall effect, that current will result in directed flow of positively charged particles in the directions shown in Fig. 1 and directed flow of negatively charged particles in the opposite direction. Our goal in this paper is to make an estimate of the order of magnitude of the resulting charge-dependent v_1 in the final state pions and (anti)protons. We will make many simplifying assumptions, since our goal is only to show which v_1-correlations can be used to look for effects of the initial magnetic field and to give experimentalists an order-of-magnitude
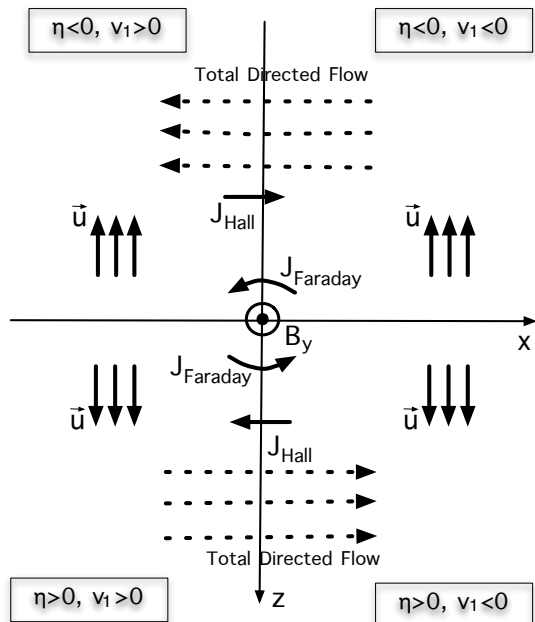
FIG. 1: Schematic illustration of how the magnetic field $\vec{B}$ in a heavy ion collision results in a directed flow, v_1, of electric charge. The collision occurs in the z-direction, meaning that the longitudinal expansion velocity $\vec{u}$ of the conducting QGP that is produced in the collision points in the $+z$ ($-z$) direction at positive (negative) z. We take the impact parameter vector to point in the x direction, choosing the nucleus moving toward positive (negative) z to be located at negative (positive) x, which is to say taking the magnetic field $\vec{B}$ to point in the $+y$ direction. The direction of the electric currents due to the Faraday and Hall effects is shown, as is the direction of the directed flow of positive charge (dashed) in the case where the Faraday effect is on balance stronger than the Hall effect. In some regions of spacetime, the electric current due to the Hall effect is greater than that due to the Faraday effect; in other regions, the Faraday-induced current is stronger. The computation of the directed flow of charged particles is a suitably weighted integral over spacetime, meaning that the final result for the directed flow arises from a partial cancellation between the opposing Faraday and Hall effects. In some settings (i.e. for some hadron species, with momenta in some ranges) the total directed flow for positively charged particles points as shown. In other settings, it points in the opposite direction.

sense of how large these correlations may reasonably be expected to be.

The biggest simplifying assumption that we shall make is to treat the electrical conductivity of the QGP σ as if it were a constant. We make this assumption only because it will permit us to do a mostly analytic calculation. In reality, σ is certainly temperature dependent: just on dimensional grounds it is expected to be proportional to the temperature of the plasma. This means that σ should certainly be a function of space and time as the plasma expands and flows hydrodynam-

ically, with σ decreasing as the plasma cools. Furthermore, during the early pre-equilibrium epoch σ should rapidly increase from zero to its equilibrium value. Taking all this into consideration would require a full, numerical, magnetohydrodynamic analysis, which we leave to the future. We shall treat σ as a constant, unchanging until freezeout. We select a reasonable order-of-magnitude value of the conductivity σ based upon recent lattice calculations [22–26]. It is conventional in these calculations to quote results for $C_{em}^{-1}\sigma/T$, where $C_{em} \equiv (\frac{4}{9} + \frac{1}{9} + \frac{1}{9})e^2 = 0.061$ in 3-flavor QCD. The quantity $C_{em}^{-1}\sigma/T$ is weakly temperature dependent between about $1.2T_c$ and $2T_c$, with $T_c \sim 170$ MeV the temperature of the crossover from a hadron gas to quark-gluon plasma. At $T = 1.5T_c \sim 255$ MeV, $C_{em}^{-1}\sigma/T$ lies between 0.2 and 0.4 [22–26]. We shall set $\sigma = 0.023$ fm^{-1} throughout this paper. This corresponds to $C_{em}^{-1}\sigma/T = 0.3$ at $T = 255$ MeV.

To do an analytic calculation we need an analytic solution for the hydrodynamic expansion of the conducting fluid in the absence of any electric currents. We shall use the analytic solution to relativistic viscous hydrodynamics for a conformal fluid with the shear viscosity to entropy density ratio given by $\eta/s = 1/(4\pi)$ found by Gubser in 2010 [27]. The solution describes a finite size plasma produced in a *central* collision that is obtained from conformal hydrodynamics by demanding boost invariance along the beam (i.e. z) direction, rotational invariance around z, and two special conformal invariances perpendicular to z. This leads to a fluid flow that preserves a $SO(1,1) \times SO(3) \times Z_2$ subgroup of the full 4-dimensional conformal group, with the Z_2 coming from invariance under $z \leftrightarrow -z$. Gubser obtains analytic expressions for the four-velocity u^μ from which one can construct the local temperature and energy density of the conformal fluid. As we demonstrate below, we can choose parameters such that Gubser's solution yields a reasonable facsimile of the pion and proton transverse momentum spectra observed in RHIC and LHC collisions with $20-30\%$ centrality, corresponding to collisions with a mean impact parameter between 7 and 8 fm, see e.g. [28, 29]. Gubser's hydrodynamic solution is rotationally invariant around the z-direction and so in reality cannot be directly applicable to collisions with nonzero impact parameter. A future numerical analysis should be based instead upon a numerical solution to (3+1)-dimensional relativistic hydrodynamics for non-central heavy ion collisions.

We shall assume throughout that the effects of the magnetic field are small in the sense that the velocity of charged particles that results (via Hall and Faraday) from the presence of $\vec{B}$, call it $\vec{v}$, is much smaller than the velocity of the expanding plasma $\vec{u}$. That is, we require $|\vec{v}| \ll |\vec{u}|$. We shall see that this is a good assumption. Upon making this assumption, and given that our goal is only an order-of-magnitude estimate of the magnitude of the charge-dependent directed flow, all we really need from hydrodynamics is a flow field $\vec{u}$ that is reasonable in

transverse extent and in magnitude, and a temperature field T that can be used to define a reasonable freezeout surface in spacetime at which the hydrodynamic fluid cools below some specified freezeout temperature and is replaced by hadrons, following the Cooper-Frye procedure [30]. In particular, we shall only be interested in the small charge-dependent azimuthal anisotropy v_1 due to the velocity $\vec{v}$ of charged particles and shall not be interested at all in the larger, but charge-independent, azimuthal anisotropies in the hydrodynamic expansion that are induced by the initial azimuthal anisotropy in collisions with nonzero impact parameter. For all our purposes, therefore, Gubser's azimuthally symmetric solution suffices.

In order to obtain the velocity $\vec{v}$ associated with the charged currents due to the electromagnetic field, in Section 2 we first calculate the magnetic and electric fields themselves, $\vec{B}$ and $\vec{E}$, by solving Maxwell's equations in the center-of-mass frame (the frame illustrated in Fig. 1). From $\vec{E}$ and the electrical conductivity σ it would be straightforward to obtain the electric current density $\vec{J} = \sigma\vec{E}$. However, for our purposes what we need is not $\vec{J}$ itself. The electric current $\vec{J}$ will be associated with positively charged fluid moving with mean velocity $\vec{v}$ and negatively charged fluid moving with mean velocity $-\vec{v}$, and what we need to determine is the magnitude and direction of $\vec{v}$.

In order to determine $\vec{v}$ at some point in spacetime, we first boost to the local fluid rest frame at that point in spacetime, namely the (primed) frame in which $\vec{u'} = 0$ at that point. In the primed frame all components of the electromagnetic field $\vec{E'}$ and $\vec{B'}$ are non-vanishing. We then solve the equation of motion for a charged fluid element with mass m in this frame, using the Lorentz force law and requiring stationary currents:

$$m\frac{d\vec{v'}}{dt} = q\vec{v'} \times \vec{B'} + q\vec{E'} - \mu m\vec{v'} = 0\,, \qquad (1.1)$$

where the last term describes the drag force on a fluid element with mass m on which some external (in this case electromagnetic) force is being exerted, with μ being the drag coefficient. The nonrelativistic form of (1.1) is justified by the aforementioned assumption $|\vec{v}|/|\vec{u}| \ll 1$. The calculation of μm from first principles is an interesting open question. In QCD it may be accessible via a lattice calculation; in $\mathcal{N} = 4$ supersymmetric Yang-Mills (YM) theory it should be accessible via a holographic calculation. At present its value is known precisely only for heavy quarks in $\mathcal{N} = 4$ SYM theory, in which [31–33]

$$\mu m = \frac{\pi\sqrt{\lambda}}{2}T^2\,, \qquad (1.2)$$

with $\lambda \equiv g^2 N_c$ the 't Hooft coupling, g being the gauge coupling and N_c the number of colors. For the purpose of our order-of-magnitude estimate, we shall use (1.2) with $\lambda = 6\pi$. As in our (crude) treatment of the electric conductivity σ, and as there for the purpose of obtaining

our estimates from a mostly analytic calculation, we shall also approximate μm as a constant. Throughout this paper we shall choose the constant value of μm to be that in (1.2) at $T = 1.5T_c$ with $T_c \sim 170$ MeV.

In the local fluid rest frame, we look for stationary currents for the up and down quarks and anti-quarks. We assume that the particle density for u and d quarks and antiquarks are all the same, thus neglecting any chemical potentials for baryon number or isospin. (Leaving out the strange quarks and neglecting any chemical potentials for baryon number or isospin are less serious simplifying assumptions than the others that we have already made.) With these assumptions, the average velocity for the positively charged species is $(\vec{v'}_u + \vec{v'}_{\bar{d}})/2$ and that for the negatively charged species is $(\vec{v'}_d + \vec{v'}_{\bar{u}})/2$. Having found $\vec{v'}$ for the positively charged particles (and $-\vec{v'}$ for the negatively charged particles) we next transform the four velocity v'^{μ} back to the center-of-mass frame, obtaining a four velocity, that we can denote by $V^{+\mu}$ or $V^{-\mu}$, that describes the sum (in the sense of the relativistic addition of velocities) of $\vec{u}$ and the additional charge-dependent velocity $\vec{v}$ or $-\vec{v}$. That is, the four-velocity $V^{+\mu}$ (or $V^{-\mu}$) includes both the velocity of the positively (or negatively) charged particles due to electromagnetic effects and the much larger, charge-independent, velocity $\vec{u}$ of the expanding plasma. Finally, we apply the Cooper-Frye freezeout procedure [30], taking $V^{+\mu}$ and $V^{-\mu}$ as the four-velocity for positively and negatively charged particles, integrating over the freezeout surface, and calculating the spectra of charged pions and (anti)protons as a function of the transverse momentum p_T, the azimuthal angle in momentum space ϕ_p and the momentum-space rapidity Y. Integrating the spectra against $\cos\phi_p$ yields the directed flow $v_1^+(p_T, Y)$ (and $v_1^-(p_T, Y)$) for positively (and negatively) charged particles.

After solving Maxwell's equations in Section II, in Section III we present our implementation of Gubser's solution for $\vec{u}$, including the hadron spectra that result from it after freezeout. In Section IV we present the calculation of $\vec{v}$, and from it v_1, that we have just sketched. We present our estimates of the charge-dependent v_1 for pions and protons in heavy ion collisions at the LHC and RHIC. We close in Section V with some suggested correlation observables designed to pull out the effects of the magnetic field whose magnitude we have estimated, and a look ahead.

II. COMPUTING THE ELECTROMAGNETIC FIELD

In this Section we determine the electromagnetic field in the center-of-mass frame. The magnetic field is produced by the charged ions in a non-central collision. We begin by considering a single point-like charge located at the position $\vec{x'}_\perp$ in the transverse plane moving in the $+z$ direction with velocity $\vec{\beta}$. Our coordinates are as in

Fig. 1. Using Ohm's law $\vec{J} = \sigma\vec{E}$ for the current produced in the medium, one finds the wave equations

$$\nabla^2\vec{B} - \partial_t^2\vec{B} \; - \; \sigma\partial_t\vec{B} =$$
$$-e\beta\nabla \times \left[\hat{z}\delta(z - \beta t)\delta(\vec{x}_\perp - \vec{x'}_\perp)\right], \; (2.1)$$
$$\nabla^2\vec{E} - \partial_t^2\vec{E} \; - \; \sigma\partial_t\vec{E} = -e\nabla\left[\delta(z - \beta t)\delta(\vec{x}_\perp - \vec{x'}_\perp)\right] +$$
$$e\beta\hat{z}\partial_t\left[\delta(z - \beta t)\delta(\vec{x}_\perp - \vec{x'}_\perp)\right]. \quad (2.2)$$

Solution of these equations is straightforward by the method of Green functions. We evaluate the y-component of $\vec{B}$ at an arbitrary spacetime point $(t, z, \vec{x}_\perp)$ in the forward lightcone, $t > |z|$. We shall write the spacetime point in terms of its proper time $\tau \equiv \sqrt{t^2 - z^2}$ and spacetime rapidity $\eta \equiv \operatorname{arctanh}(z/t)$ as well as $x_\perp \equiv |\vec{x}_\perp|$ and the azimuthal angle ϕ. We find that B_y due to a $+$ mover at location $\vec{x'}_\perp$ and $z' = \beta t$ is given by

$$eB_y^+(\tau, \eta, x_\perp, \phi) \; = \; \alpha\sinh(Y_b)(x_\perp\cos\phi - x'_\perp\cos\phi')$$
$$\frac{(\frac{\sigma|\sinh(Y_b)|}{2}\sqrt{\Delta} + 1)}{\Delta^{\frac{3}{2}}}e^A, \quad (2.3)$$

where $\alpha = e^2/(4\pi)$ is the electromagnetic coupling, $Y_b \equiv \operatorname{arctanh}(\beta)$ is the rapidity of the $+$ mover, and we have defined

$$A \equiv \frac{\sigma}{2}\left(\tau\sinh(Y_b)\sinh(Y_b - \eta) - |\sinh(Y_b)|\sqrt{\Delta}\right)(2.4)$$
$$\Delta \equiv \tau^2\sinh^2(Y_b - \eta) + x_\perp^2 + x'^2_\perp$$
$$-2x_\perp x'_\perp\cos(\phi - \phi'). \quad (2.5)$$

We were able to obtain this analytic solution because we are treating σ as constant, throughout all space and time, with the value $\sigma = 0.023$ fm^{-1} chosen as described in Section I. The finite size and finite duration of the fluid of interest will enter our calculation in Section III, via the calculation of the freezeout surface. As a check, note that upon setting $\sigma = 0$ in (2.3) one recovers the standard result for B_y in vacuum, as in Ref. [1].

A similar calculation shows the x-component of the electric field produced by the $+$ moving particle is given by

$$eE_x^+(\tau, \eta, x_\perp, \phi) = eB_y^+(\tau, \eta, x_\perp, \phi)\coth(Y_b - \eta). \,(2.6)$$

The other components of the electromagnetic field will turn out to be irrelevant.

Now we need to evaluate the total B_y and E_x fields produced by all the protons in the two colliding nuclei, some of which are spectators, meaning that at their $\vec{x'}_\perp$ location one finds either $+$ movers or $-$ movers but not both, and others of which are participants, meaning that at their locations one has both $+$ and $-$ movers. The spectators have the same rapidity after the collision as they did before it, referred to as beam rapidity and denoted Y_0. (At RHIC, $Y_0 \simeq 5.4$ and at the LHC, $Y_0 \simeq 8$.)

Because the participant protons lose some rapidity in the collision, after the collision they have some distribution of rapidities Y_b. We shall use the empirical distribution [1, 34]

$$f(Y_b) = \frac{a}{2\sinh(aY_0)}e^{aY_b}, \qquad -Y_0 \le Y_b \le Y_0\,, \; (2.7)$$

for the $+$ moving participants, choosing $a \approx 1/2$ for both RHIC and LHC collisions. (This value of a corresponds to the string junction exchange intercept in Regge theory [34] and is consistent with experimental data on baryon stopping [34, 35].) After the collision the $-$ moving participants have the same distribution with Y_b replaced by $-Y_b$. We must then add up the B_y and E_x produced by all the spectators and participants. Denoting the magnetic field due to spectators and participants moving in the $+$(-) z direction by $\vec{B}_s^+$ $(\vec{B}_s^-)$ and $\vec{B}_p^+(\vec{B}_p^-)$, the total magnetic field will be given by $\vec{B} = \vec{B}_s^+ + \vec{B}_s^- + \vec{B}_p^+ + \vec{B}_p^-$.

Let us first look at the contribution from the spectators. We shall make the simplifying assumption that the protons in a nucleus are uniformly distributed within a sphere of radius R, with the centers of the spheres located at $x = \pm b/2$, $y = 0$ and moving along the $+z$ and $-z$ directions with velocity β. We shall take $R = 7$ fm and $b = 7$ fm. If we project the probability distribution for the protons in either the $+$ moving or the $-$ moving nucleus onto the transverse plane it takes the form

$$\rho_\pm(x_\perp) = \frac{3}{2\pi R^3}\sqrt{R^2 - \left(x_\perp^2 \pm b\,x_\perp\cos(\phi) + \frac{b^2}{4}\right)}.(2.8)$$

In a collision with impact parameter $b \ne 0$ the $+$ and $-$ moving spectators are each located in a crescent-shaped region of the $\vec{x'}_\perp$-plane and one can write the total electromagnetic field produced by all the spectators as [1]

$$eB_{y,s} \; = \; -Z\int_{-\frac{\pi}{2}}^{\frac{\pi}{2}}d\phi'\int_{x_{\text{in}}(\phi')}^{x_{\text{out}}(\phi')}dx'_\perp x'_\perp\rho_-(x'_\perp) \quad (2.9)$$
$$\times\left(eB_y^+(\tau, \eta, x_\perp, \pi - \phi) + eB_y^+(\tau, -\eta, x_\perp, \phi)\right),$$
$$eE_{x,s} \; = \; Z\int_{-\frac{\pi}{2}}^{\frac{\pi}{2}}d\phi'\int_{x_{\text{in}}(\phi')}^{x_{\text{out}}(\phi')}dx'_\perp x'_\perp\rho_-(x'_\perp) \quad (2.10)$$
$$\times\left(-eE_x^+(\tau, \eta, x_\perp, \pi - \phi) + eE_x^+(\tau, -\eta, x_\perp, \phi)\right),$$

with B_y^+ and E_x^+ defined in (2.3) and (2.6). Here x_{in} and x_{out} are the endpoints of the $x'_\perp$ integration regions that define the crescent-shaped loci where one finds either $+$ movers or $-$ movers but not both. They are given by

$$x_{\text{in/out}}(\phi') = \mp\frac{b}{2}\cos(\phi') + \sqrt{R^2 - \frac{b^2}{4}\sin^2(\phi')}. \,(2.11)$$

We have taken $Z = 79$ and $Z = 82$ for heavy ion collisions at RHIC and the LHC, respectively. In Fig. 2 we plot eB_y produced by the spectators at the center of a heavy ion collision at the LHC. We see that, as other authors have
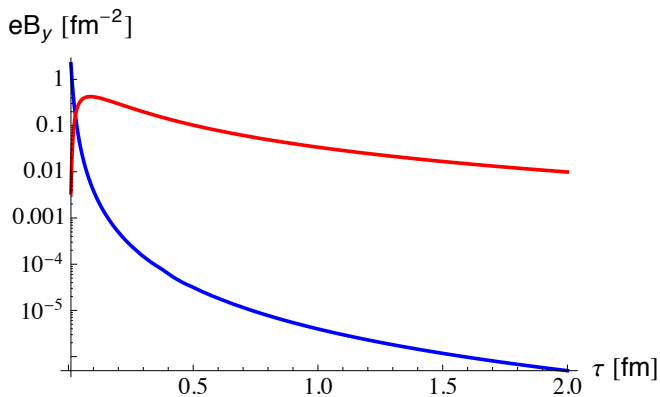
FIG. 2: Magnetic field B_y perpendicular to the reaction plane produced by the spectators in a heavy ion collision with impact parameter $b = 7$ fm at the LHC. The value of eB_y at the center of the collision, at $\eta = 0 = x_\perp$, is plotted as a function of τ. The blue curve shows how rapidly B_y at $\eta = 0 = x_\perp$ would decay as the spectators recede if there were no medium present, i.e. in vacuum with $\sigma = 0$. The presence of a conducting medium with $\sigma = 0.023$ fm^{-1} substantially delays the decay of B_y (red curve). At very early times before any medium has formed, when the blue curve is well above the red curve the blue curve is a better approximation. We shall use the red curve throughout, though, because our calculation is not sensitive to these earliest times.

shown previously (see Refs. [2–7], in particular Fig. 4 in Ref. [6]) the presence of the conducting medium delays the decrease in the magnetic field. This is Faraday's Law in action, and it tells us that an electric current, indicated schematically by J_{Faraday} in Fig. 1, has been induced in the plasma. Our goal in subsequent Sections will be to estimate the observable consequences of the presence of such a current.

A similar calculation to that for the spectators shows that the total contribution to B_y and E_x from the participants is given by

$$eB_{y,p} = -Z \int_{-Y_0}^{Y_0} dY_b f(Y_b) \int_{-\frac{\pi}{2}}^{\frac{\pi}{2}} d\phi' \int_0^{x_{\text{in}}(\phi')} dx'_\perp x'_\perp \rho_-(x'_\perp)$$
$$\times \left(eB_y^+(\tau, \eta, x_\perp, \pi - \phi) + eB_y^+(\tau, -\eta, x_\perp, \phi) \right), \quad (2.12)$$

$$eE_{x,p} = Z \int_{-Y_0}^{Y_0} dY_b f(Y_b) \int_{-\frac{\pi}{2}}^{\frac{\pi}{2}} d\phi' \int_0^{x_{\text{in}}(\phi')} dx'_\perp x'_\perp \rho_-(x'_\perp)$$
$$\times \left(-eE_x^+(\tau, \eta, x_\perp, \pi - \phi) + eE_x^+(\tau, -\eta, x_\perp, \phi) \right), (2.13)$$

where the integration regions have been chosen to correspond to the almond-shaped locus in the transverse plane where one finds both + and − movers. Finally, the total electromagnetic field is given by the sum of the contribution of the spectators in (2.9), (2.10) and the participants in (2.12), (2.13). The other components of the electromagnetic field will be irrelevant because $B_z = 0$. In most, but not all, locations in spacetime the contribution of the participant protons to both B_y and E_x is substantially

smaller than that of the spectators. We have checked that eliminating the contribution from the participants changes the final results that we obtain below for the directed flow by at most 10%, typically much less.

III. HYDRODYNAMICS AND FREEZEOUT

As we have already noted in Section I, we shall use the analytic solution to the equations of relativistic viscous conformal hydrodynamics found recently by Gubser [27] that describes the boost invariant longitudinal expansion and the hydrodynamic transverse expansion of a circularly symmetric blob of strongly coupled conformal plasma with four-velocity $u^\mu(\tau, \eta, x_\perp)$, independent of the azimuthal angle ϕ. We shall then place this hydrodynamic solution in the electric and magnetic fields computed in Section II, and determine the small additional charge-dependent velocity $\vec{v}$ that results. We refer to Ref. [27] for details of Gubser's solution and confine ourselves here to a brief summary. The only nonzero components of u^μ are u^τ, which describes the boost-invariant longitudinal expansion, and $u^\perp$, which describes the transverse expansion. They are given by [27]

$$u^\tau = \frac{1 + q^2\tau^2 + q^2 x_\perp^2}{2q\tau\sqrt{1+g^2}}, \qquad u^\perp = \frac{qx_\perp}{\sqrt{1+g^2}}, \quad (3.1)$$

where

$$g \equiv \frac{1 + q^2 x_\perp^2 - q^2\tau^2}{2q\tau}. \quad (3.2)$$

The fluid four-velocity u^μ in the solution is specified by a single parameter denoted by q, with the dimension of $1/\text{length}$. (q is unrelated to charge.) The transverse size of the plasma is proportional to $1/q$. The local temperature of the plasma is then given by [27]

$$T = \frac{1}{\tau f_*^{1/4}} \left(\frac{\hat{T}_0}{(1+g^2)^{1/3}} + \frac{\text{H}_0\, g}{\sqrt{1+g^2}} \right.$$
$$\left. \times \left[1 - (1+g^2)^{1/6}{}_2F_1\left(\frac{1}{2}, \frac{1}{6}; \frac{3}{2}; -g^2\right) \right] \right), (3.3)$$

where the first the term, proportional to the dimensionless parameter $\hat{T}_0$, corresponds to an ideal fluid and the second term incorporates dissipative effects due to the shear viscosity η. The initial temperature of the plasma is proportional to the parameter $\hat{T}_0$, and is also affected by the choice of the parameter q. The expression (3.3) introduces two further dimensionless parameters that we shall choose as in Ref. [27]. f_* is the parameter that relates the energy density of the plasma ε to the local temperature, $\varepsilon = f_* T^4$, and we shall choose the value $f_* = 11$, reasonable for the QCD quark-gluon plasma with $T \sim 300$ MeV [36]. H_0 is the parameter that controls the strength of viscous corrections; it is defined by $\eta = H_0\, \varepsilon^{3/4}$. We choose the value $H_0 = 0.33$ that corresponds to $\eta/s = 0.134$, as has been estimated for $SU(3)$

gluodynamics [37]. The local energy density ε and the fluid four-velocity u^μ fully specify the energy-momentum tensor of the fluid.

It remains to fix the parameters q and $\hat{T}_0$. Together they determine the initial temperature profile of the plasma at some fiducial early time that should be comparable to or greater than the time at which a hydrodynamic description becomes valid. Hydrodynamic calculations appropriate for heavy ion collisions at the LHC, for example those in Refs. [38], suggest that at $\tau = 0.6$ fm the initial temperature should be between 445 MeV and 485 MeV. It is not possible to use this initial temperature to fix q or $\hat{T}_0$, however, because the the temperature profile as a function of $x_\perp$ is quite different in Gubser's solution than in a heavy ion collision: in Gubser's solution the temperature profile is both more peaked at $x_\perp = 0$ and has a heavier large-$x_\perp$ tail relative to a Woods-Saxon distribution with its flat middle and damped tails. The parameters q and $\hat{T}_0$ also implicitly determine the radial velocity profile at the end of the hydrodynamic evolution, which in turn determines the hadron spectra after freezeout. Our approach, therefore, is to explore the two parameter space looking for values that give reasonable final state spectra to mock up heavy ion collisions at the LHC in the 20 - 30% centrality class (i.e. the collisions in the 20th-30th percentile in impact parameter, which have impact parameters around $7 - 8$ fm. We have found that choosing $\hat{T}_0 = 10.8$ and $q^{-1} = 6.4$ fm yields reasonable pion and proton spectra, as we shall show below. This choice yields a temperature of 617 MeV at the center of the collision at $\tau = 0.6$ fm and an average temperature within $x_\perp < 7$ fm at $\tau = 0.6$ fm of 458 MeV. For heavy ion collisions at RHIC we find instead that choosing $\hat{T}_0 = 7.5$ and $q^{-1} = 5.3$ fm yields reasonable pion and proton spectra. With this choice, at $\tau = 0.6$ fm the temperature at $x_\perp = 0$ is 488 MeV and the average temperature within $x_\perp < 7$ fm is 326 MeV.

We calculate the hadron spectra for the pions and the protons by applying the Cooper-Frye freezeout procedure to Gubser's hydrodynamic solution. The hadron spectrum for particles of species i with mass m_i will depend on transverse momentum p_T, momentum space rapidity Y and the azimuthal angle in momentum space ϕ_p. These are related to p^μ by

$$
\begin{aligned}
p^0 &= m_T \cosh Y, \\
p^z &= m_T \sinh Y, \\
p^y &= p_T \sin \phi_p, \\
p^x &= p_T \cos \phi_p,
\end{aligned}
\tag{3.4}
$$

where we have defined the transverse mass $m_T \equiv \sqrt{p_T^2 + m_i^2}$. To establish notation, note that the dependence of the hadron spectrum on ϕ_p can be expanded as

$$
\begin{aligned}
S_i &\equiv p^0 \frac{d^3 N_i}{dp^3} = \frac{d^3 N_i}{p_T dY \, dp_T d\phi_p} \\
&= v_0 \left(1 + 2\, v_1 \cos(\phi_p - \pi) + 2\, v_2 \cos 2\phi_p + \cdots \right),
\end{aligned}
\tag{3.5}
$$

where in general the parameters v_n will depend on Y and p_T. Note that the sign of v_1 is conventionally defined such that if the spectators moving toward positive z, i.e. moving with positive Y, were deflected away from the center of the collision that would correspond to a positive v_1. We see in Fig. 1 that, with our choices of conventions, the spectators moving toward positive z are at negative x. This means that for us $v_1 > 0$ corresponds to directed flow toward negative x, as we have already indicated in the labelling of Fig. 1. This is why v_1 multiplies $\cos(\phi_p - \pi)$, not $\cos\phi_p$, in (3.5).

Gubser's solution is boost invariant and azimuthally symmetric, meaning that it is independent of Y and ϕ_p. In this case, the only nonvanishing v_n is v_0, and $v_0 = (2\pi p_T)^{-1} d^2 N / dY \, dp_T$ depends only on p_T. We want to calculate v_0 for pions and protons. The standard prescription to obtain the hadron spectra from a hydrodynamic flow, assuming sudden freezeout when the fluid cools to a specified freezeout temperature T_f, was developed by Cooper and Frye [30]. We shall take $T_f = 130$ MeV for heavy ion collisions at both the LHC and RHIC. The freezeout surface is the isothermal surface in spacetime at which the temperature of Gubser's hydrodynamic solution, given in (3.3), satisfies $T(x_\perp, \tau) = T_f$. The spectrum for hadrons of species i is then given by [30]

$$
S_i = p^0 \frac{d^3 N_i}{dp^3} = -\frac{g_i}{(2\pi)^3} \int d\Sigma_\mu \, p^\mu F\left(-\frac{p^\mu u_\mu}{T_f} \right), \tag{3.6}
$$

where $d\Sigma_\mu$ is the area element on the freezeout surface, u^μ is the 4-velocity of the fluid, g_i is the degeneracy of hadron species i and $F(x)$ is a distribution function that we will take as the Boltzmann distribution $F(x) = \exp(-x)$. As with many of our other simplifying assumptions, we choose Boltzmann rather than Fermi-Dirac or Bose-Einstein in order to obtain a calculation that can be done mostly analytically. (The sign in the argument of F in (3.6) comes from our use of the mostly + signature metric.) The freezeout surface is $\Sigma^\mu = (\tau_f(x_\perp), \eta, x_\perp, \phi)$ where $\tau_f(x_\perp)$ is the solution of the equation $T(x_\perp, \tau_f) = T_f$. See Fig. 3 (top). The area element perpendicular to the freezeout surface is

$$
\begin{aligned}
d\Sigma_\mu &= -\epsilon_{\mu\nu\lambda\rho} \frac{\partial \Sigma^\nu}{\partial \eta} \frac{\partial \Sigma^\lambda}{\partial x_\perp} \frac{\partial \Sigma^\rho}{\partial \phi} \sqrt{-g} \, d\eta \, dx_\perp d\phi \\
&= (-1, 0, -R_f, 0) \, x_\perp \tau_f \, d\eta \, dx_\perp d\phi,
\end{aligned}
\tag{3.7}
$$

where $\sqrt{-g} = x_\perp \tau$ on the freezeout surface and where we have used the fact that $dT = (\partial T / \partial x_\perp) dx_\perp + (\partial T / \partial \tau) d\tau = 0$ on the freezeout surface to define

$$
R_f \equiv -\frac{\partial \tau}{\partial x_\perp} = \frac{\partial T}{\partial x_\perp} \bigg/ \frac{\partial T}{\partial \tau} \bigg|_{T_f}. \tag{3.8}
$$

This completes the specification of the quantities appearing in the expression (3.6) for the hadron spectra.

We now calculate (3.6) for Gubser's flow, for example with the parameters chosen with LHC heavy ion collisions in mind as we described above. For u^μ as in Gubser's flow, the argument of the function F simplifies as

$$
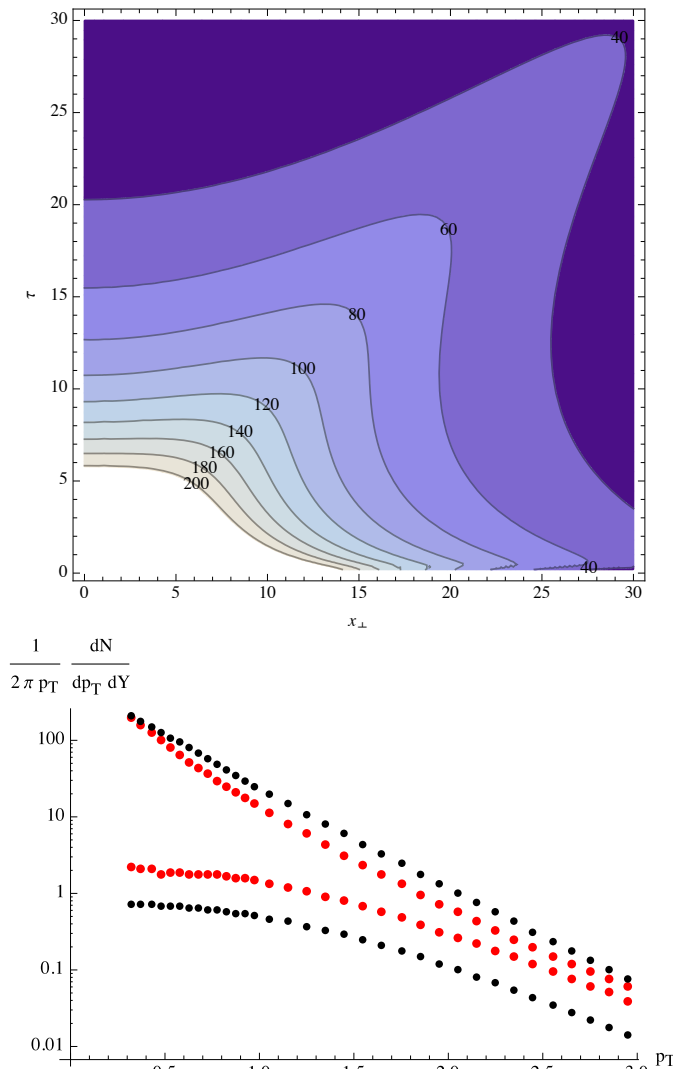p^\mu u_\mu = -m_T u^\tau \cosh(Y - \eta) + p_T u^\perp \cos(\phi_p - \phi). \tag{3.9}
$$

alytically, obtaining

$$
\left. p^0 \frac{d^3 N_i}{dp^3} \right|_G = \frac{g_i}{2\pi^2} \int dx_\perp x_\perp \, \tau_f(x_\perp)
$$

$$
\times \left\{ m_T \, K_1 \left(\frac{m_T u^\tau}{T_f} \right) I_0 \left(\frac{p_T u^\perp}{T_f} \right) \right.
$$

$$
\left. + R_f p_T K_0 \left(\frac{m_T u^\tau}{T_f} \right) I_1 \left(\frac{p_T u^\perp}{T_f} \right) \right\} \quad (3.10)
$$

where R_f was defined in (3.8). As expected, the result is independent of Y and ϕ_p and only depends on p_T. One then evaluates the $x_\perp$ integral on the freezeout surface numerically and obtains the spectra of hadrons freezing out from Gubser's hydrodynamic flow as a function of p_T. The results for the charged pion and proton spectra are presented in Fig. 3 (bottom).

We observe that Gubser's flow with this choice of parameters does not yield fully satisfactory spectra — in particular there are too few protons relative to pions — but at a qualitative level it reproduces many features of the spectra in LHC heavy ion collisions with 20-30% centrality measured using the ALICE detector [39]. The shortfall in the number of protons comes because we are using a single freezeout temperature T_f instead of letting the number of each hadron species, for example protons, freezeout first at a somewhat higher chemical freezeout temperature or using a hadron cascade code between T_c and T_f. By assuming thermal and chemical equilibrium and using hydrodynamics all the way down to a single freezeout temperature $T_f = 130$ MeV the proton multiplicity in the final state is being overly suppressed by the Boltzmann factor at $T = T_f$. We see, though, that the shape of the proton spectrum is reproduced well. If we were to use a slightly lower T_f, say 120 or 110 MeV, we could improve the shape of the pion spectrum at the expense of suppressing the proton multiplicity even more than in Fig. 3. Given the simplicity, and the unphysical initial temperature profile, of Gubser's analytic hydrodynamic solution and given the crude freezeout at a single T_f that we are employing, we find it impressive that it is possible to obtain spectra as reasonable as those in Fig. 3.

We have also done the exercise of comparing spectra obtained at freezeout from Gubser's hydrodynamic solution with varying values of q and $\hat{T}_0$ to pion and proton spectra for 20-30% centrality heavy ion collisions at RHIC [40], finding reasonable spectra upon choosing $q^{-1} = 5.3$ fm and $\hat{T}_0 = 7.5$, values of the parameters that we already quoted earlier in this Section.

In the next Section, after we have determined the charge-dependent velocity corresponding to the electric current we shall re-evaluate (3.6) upon replacing u^μ by $V^{+\mu}$ or $V^{-\mu}$ for positively or negatively charged hadrons.

FIG. 3: Features of Gubser's flow. Top figure illustrates the isothermal curves in the $(x_\perp, \tau)$ plane for Gubser's hydrodynamic solution with the parameters $\hat{T}_0 = 10.8$ and $q^{-1} = 6.4$ fm. We choose the $T = 130$ MeV isotherm as the freezeout surface. Bottom figure is the comparison of the spectrum of positively charged pions (black, top) and protons (black, bottom) as a function of transverse momentum p_T resulting from Gubser's hydrodynamic solution to the spectra for pions (red, top) and protons (red, bottom) in LHC heavy ion collisions with 20-30% centrality measured by the ALICE collaboration, as in Ref. [39]. Because we have no chemical potential for baryon number or isospin in our calculation, the spectra of antiprotons and protons are identical as are the spectra of the negatively and positively charged pions.

One can then perform the η and ϕ integrals in (3.6) an-

IV. ELECTRIC CURRENT AND CHARGE-DEPENDENT DIRECTED FLOW

We are now ready to study the effects of the magnetic field on the directed flow v_1, which is the purpose of this paper. In the center-of-mass frame, the magnetic and electric fields are given by the sum of (2.9) and (2.12), and (2.10) and (2.13). The fluid velocity in the absence of any electromagnetic effects is given by u^μ in Gubser's solution, (3.1). In order to obtain the fluid velocity V^μ, including electromagnetic effects, at a given spacetime point we first Lorentz transform by $\Lambda(-\vec{u})$ to the local fluid rest frame in which $\vec{u'} = 0$ at that point and then use the Lorentz transformed electromagnetic fields in the stationary current condition (1.1), setting $q = +2e/3$ to obtain $\vec{v'}_u$, setting $q = +e/3$ to obtain $\vec{v'}_{\bar{d}}$, and averaging these to obtain $\vec{v'}$. The average drift velocity for negatively charged particles in the local fluid rest frame is obtained similarly and is given by $-\vec{v'}$. We then Lorentz transform by $\Lambda(\vec{u})$ back to the center-of-mass frame, obtaining the total velocity $V^{+\mu}$ and $V^{-\mu}$ for positively and negatively charged particles via Lorentz transforming $\vec{v'}$ and $-\vec{v'}$ back to the center-of-mass frame, respectively.

At this point we checked whether our assumption $|\vec{v}|/|\vec{u}| \ll 1$ is indeed satisfied. In order to characterize this assumption in a Lorentz invariant fashion, we can calculate the difference between the Lorentz factor for the total velocity $V^{\pm\mu}$, including Gubser's u^μ and the excess velocity due to magnetic effects, and the Lorentz factor for u^μ alone. The difference between these turns out to be very small, of order 0.001 or smaller everywhere in the $(\eta, x_\perp, \phi)$ space.

Once we have obtained the total velocity $V^{\pm\mu}$ we can use the freezeout procedure described in the previous Section to calculate the hadron spectra including electromagnetic effects by replacing u^μ in (3.6) by $V^{+\mu}$ when evaluating the π^+ and proton spectra and by $V^{-\mu}$ when evaluating the π^- and antiproton spectra. The change to the ϕ-integrated dN/dp_T, i.e. the change to v_0 defined in (3.5), that results from using $V^{\pm\mu}$ instead of u^μ is minuscule, and for all practical purposes it is fine to use results for v_0 obtained as in Section III. Because the magnetic field induces an electric current that circulates in the (x, z) plane, see Fig. 1, when we use $V^{+\mu}$ or $V^{-\mu}$ in (3.6) we obtain a small, but nonzero, directed flow v_1 that is opposite in sign for positively and negatively charged particles. Teasing out this charge-dependent v_1 is the goal of this paper. From its definition in (3.5) we see that v_1 is given by

$$v_1(p_T, Y) = \frac{\int_{-\pi}^{\pi} d\phi_p \, \cos(\phi_p - \pi) \, S_i(p_T, Y, \phi_p)}{2\pi v_0} . \quad (4.1)$$

Recall from Fig. 1 that our conventions are such that a positive v_1 corresponds to directed flow in the negative x direction. In evaluating the denominator in (4.1) we shall use v_0 obtained from u^μ as in Section III. There are four integrals to be evaluated in the numerator of (4.1),
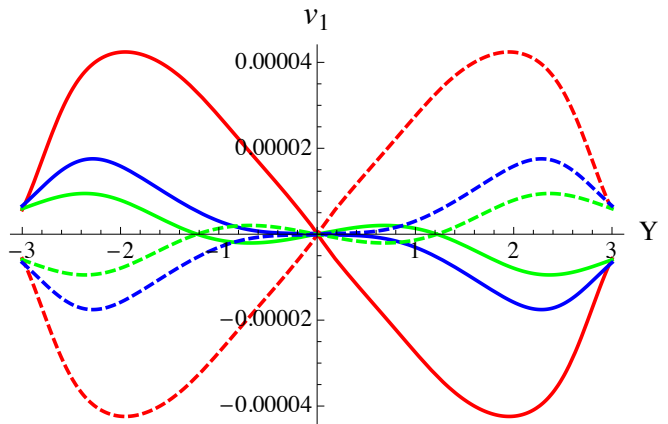

FIG. 4: Directed flow v_1 for positively charged pions (solid curves) and negatively charged pions (dashed curves) in our calculation with parameters chosen to give a reasonable facsimile of 20-30% centrality heavy ion collisions at the LHC. We plot our results for v_1 as functions of momentum-space rapidity Y at $p_T = 0.25$ (green), 0.5 (blue) and 1 GeV (red). Here and in all subsequent figures we are only plotting the charge-dependent contribution to the directed flow v_1 that originates from the presence of the magnetic field in the collision and that is caused by the Faraday and Hall effects. This charge-dependent contribution to v_1 must be added to the, presumably larger, charge-independent v_1. For example, if the charge-independent v_1 for pions with $Y < 0$ and $p_T = 1$ GeV is positive then in that kinematic regime our results correspond to a positive v_1 for both π^+ and π^-, with $v_1(\pi^+) > v_1(\pi^-)$.

namely integrals over $x_\perp$, η, ϕ and ϕ_p. It turns out that one can evaluate the ϕ_p integral analytically in terms of Bessel and hypergeometric functions:

$$\int_{-\pi}^{\pi} d\phi_p \, \cos\phi_p \, S_i(p_T, Y, \phi_p) = \frac{g_i}{(2\pi)^2} \int d\eta \, dx_\perp \, d\phi \, x_\perp \, \tau_f(x_\perp)$$

$$\times \; e^{-\frac{m_T}{T_f}[V^\tau \cosh(Y-\eta) - V^\eta \tau_f \sinh(Y-\eta)]}$$

$$\times \left\{ \left(V^\perp \cos\phi - x_\perp V^\phi \sin\phi \right) \right.$$

$$\times \left[\frac{m_T \cosh(Y-\eta)}{\sqrt{W}} I_1\left(\frac{p_T}{T_f}\sqrt{W}\right) \right.$$

$$\left. + R_f \, p_T \frac{v^\perp}{W}\left(I_0\left(\frac{p_T}{T_f}\sqrt{W}\right) - \Psi_2\left(\frac{p_T^2}{4T_f^2}W\right) \right) \right]$$

$$\left. + \frac{1}{2} R_f \, p_T \cos\phi \, \Psi_2\left(\frac{p_T^2}{4T_f^2}W\right) \right\}, \quad (4.2)$$

where we have defined $W \equiv (V^\perp)^2 + x_\perp^2 (V^\phi)^2$. The three remaining integrals in (4.2) have to be done numerically. After doing so we obtain $v_1(Y, p_T)$ from (4.1).

Figure 4 shows v_1 for positively and negatively charged pions as a function of momentum-space rapidity Y at transverse momenta $p_T = 0.5$, 1, and 2 GeV. In this Figure we have chosen the initial magnetic field created by
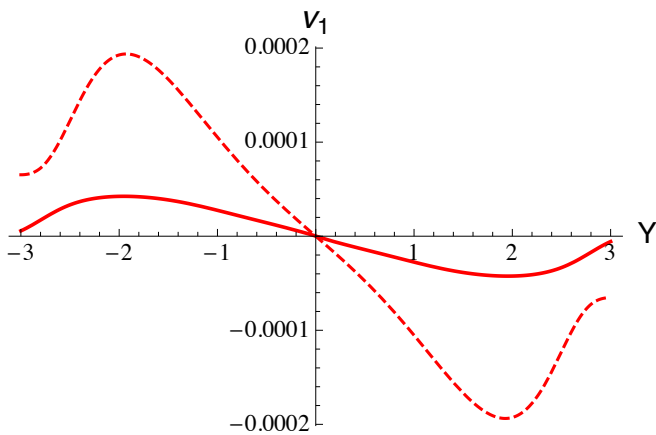
FIG. 5: Comparison of Hall vs. Faraday effects. We plot v_1 at $p_T = 1$ GeV as a function of Y for positively charged pions with values of parameters chosen as in Fig. 4, appropriate for LHC collisions. The dashed red curve is obtained if we turn off the Hall effect, keeping only the Faraday effect. The solid red curve, which is the same as that in Fig. 4, includes both the Hall and Faraday effects. We see that the Hall and Faraday effects have opposite sign, as in Fig. 1. Here, the Faraday effect is stronger.
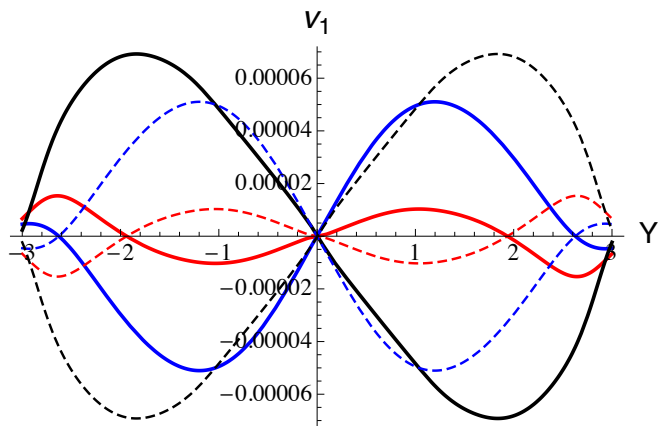

FIG. 6: v_1 for protons (solid curves) and antiprotons (dashed curves) in our calculation with the same parameters as in Fig. 4, namely parameters chosen with 20-30% centrality heavy ion collisions at the LHC in mind. We plot v_1 as a function of momentum space rapidity Y at $p_T = 0.5$ (blue), 1 (red) and 2 GeV (black).

the spectators with beam rapidity $\pm Y_0 = \pm 8$ and the participants, we have set the parameters specifying Gubser's hydrodynamic solution to $\hat{T}_0 = 10.8$ and $q^{-1} = 6.4$ fm, we have chosen the electric conductivity $\sigma = 0.023$ fm^{-1} and the drag parameter μm in (1.1) as in (1.2) with $T = 255$ MeV, and we have set the freezeout temperature to $T_f = 130$ MeV. As we have described in previous Sections, these parameters have been chosen to give a reasonable characterization of v_1 in 20-30% centrality heavy ion collisions at the LHC. Note that here and in the following we will only look at the directed flow at values of $|Y|$ that are well below Y_0. This is because the trajectories of final-state hadrons produced near beam rapidity can be affected by Coulomb interactions with the charged spectators at very late times [41], long after freezeout, and we are neglecting these effects.

We see in Fig. 1 that if the current induced by Faraday's law is greater than that induced by the Hall effect, we expect $v_1 > 0$ for negative pions at $Y > 0$ and for positive pions at $Y < 0$ and we expect $v_1 < 0$ for positive pions at $Y > 0$ and for negative pions at $Y < 0$. Comparing to Fig. 4, we observe that this is indeed the pattern for pions with $p_T = 1$ GeV, meaning that in the competition between the Faraday and Hall effects, the effect of Faraday on pions with $p_T = 1$ GeV is greater than the effect of Hall. However, the effects of Hall and Faraday on pions with smaller p_T and small Y are comparable in magnitude, for example with the Hall effect just larger for $p_T = 0.25$ and $|Y| < 1.2$, resulting in a reversal in the sign of v_1 in this kinematic range.

We can check that the Faraday and Hall effects make contributions with opposite sign to the directed flow v_1, as illustrated schematically in Fig. 1. In order to calcu-

late the contribution to v_1 that is caused by the magnetic field only via Faraday's law we proceed as follows. We solve for the electric and magnetic fields in the center-of-mass frame, as always. The electric field E_x is that due to Faraday's law: it is present because B_y is decreasing with time. So, we compute a drift velocity $\vec{v}$ (or $-\vec{v}$) for positively (or negatively) charged particles by solving $q\vec{E} = \mu m \vec{v}$ in the center-of-mass frame. At each point in space time we then add this $\vec{v}$ (and $-\vec{v}$) to the charge-independent flow velocity $\vec{u}$ using special relativistic addition of velocities, and form a four-velocity from the sum. In this way we obtain $V^{+\mu}$ (and $V^{-\mu}$) that include the velocity from Gubser's flow as well as the additional velocity for positively (and negatively) charged particles that is induced by Faraday's law. But, we have left out the Hall effect. We can then compute v_1. In Fig. 5 we show v_1 for pions with $p_T = 1$ GeV in our calculation with parameters appropriate for LHC collisions. The solid curve is the full result, including both the Hall and Faraday effects. The dashed curve shows the v_1 due only to Faraday, with the Hall effect turned off. We see that the full result arises from a partial cancellation between the Hall and Faraday effects, which act in opposite directions as in Fig. 1. For pions with $p_T = 1$ GeV, the Faraday effect makes the larger contribution to v_1. We see, though, that the contribution to v_1 due to the Hall current is comparable to that arising solely from the Faraday effect. It would therefore be interesting to attempt a full-fledged magnetohydrodynamic study in which the back-reaction of this current on the magnetic field is taken into consideration. We leave this to future work.

Next, we repeat the same calculation as in Fig. 4, this time for the protons and antiprotons. In Fig. 6 we plot v_1 for (anti)protons as a function of momentum-space rapidity Y at transverse momenta $p_T = 0.25$, 0.5, and
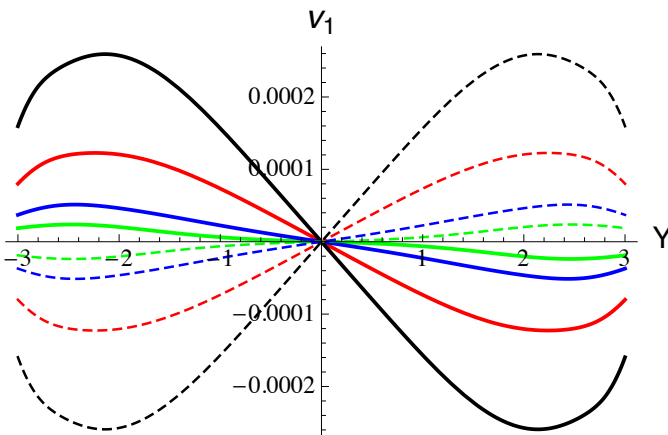
FIG. 7: v_1 for positively (solid curves) and negatively (dashed curves) charged pions with parameters chosen as for a 20-30% centrality heavy ion collision at RHIC. We plot v_1 as a function of momentum space rapidity Y at $p_T = 0.25$ (green), 0.5 (blue) 1 (red) and 2 GeV (black). Antiprotons are not displayed in this figure for visual clarity.
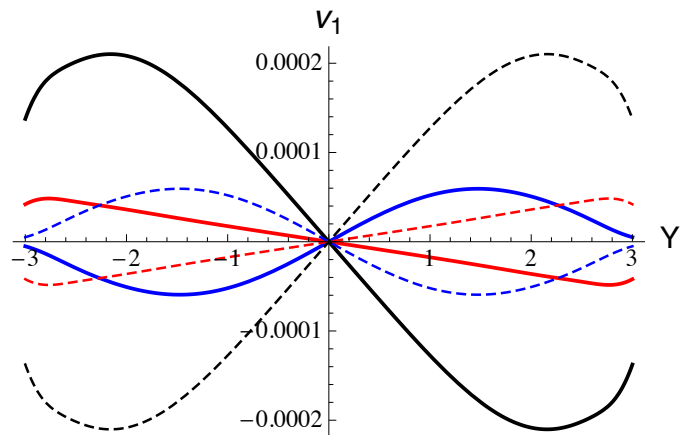
FIG. 8: v_1 for protons with parameters chosen as in Fig. 7, so as to yield estimates for RHIC. We plot v_1 as a function of Y at $p_T = 0.5$ (blue), 1 (red) and 2 GeV (black). Anti-protons are not displayed in this figure for visual clarity.

1 GeV. We observe that in the range of parameters p_T and Y that we are interested in v_1 for protons turn out to be in they opposite direction to the v_1 for pions. So, when it comes to their influence on the directed flow of protons in collisions at LHC energies, the Hall effect is stronger than the Faraday effect. How is it possible for the Faraday effect to be stronger for pions while the Hall effect is stronger for protons? First, in some regions of spacetime the electric current induced by the Faraday effect is greater than the current induced by the Hall effect whereas in other regions of spacetime the Hall current is greater. And, second, because m_T is so much larger for protons than for pions when one computes v_1 the integral (4.2) over the freezeout surface weights the contribution from different regions of the freezeout surface substantially differently for protons than for pions. Putting these together, it turns out that the Hall contribution to v_1 for protons is larger than that from the Faraday effect, whereas it is smaller for the pions.

Interestingly, the magnitude of v_1 is less for protons with $p_T = 1$ GeV than it is at lower p_T, meaning that the p_T-dependence of v_1 for protons in Fig. 6 is opposite that for pions in Fig. 4. These observations indicate that for both pions and protons the magnitude of the Faraday contribution to v_1 increases with increasing p_T faster than the magnitude of the Hall contribution.

Finally we present our estimates for heavy ion collisions at RHIC with $\sqrt{s} = 200$ AGeV and 20-30% centrality. That is, now we choose an initial magnetic field created by spectators with beam rapidity $Y_0 = 5.4$, we set the parameters specifying Gubser's hydrodynamic solution to $\hat{T}_0 = 7.5$ and $q^{-1} = 5.3$ fm, we choose the electric conductivity σ, the drag parameter μm in (1.1) and the freezeout temperature T_f as before. One change that we made is that in our calculations with these choices of pa-

rameters we left out the contribution of the participant protons to the magnetic and electric fields from the beginning, computing only the effects due to the spectators. We made this simplifying choice after having checked that, in our previous calculations with parameters appropriate for LHC collisions, leaving out the participants makes only a less than 10% difference to the calculated v_1's, in most regions of momentum space much less. In Fig. 7 we plot v_1 for positively and negatively charged pions as a function of Y at $p_T = 0.25$, 0.5, 1 and 2 GeV. We observe that Faraday effect is dominant for pions at RHIC even for p_T as low as 0.25 GeV. And, in Fig. 8 we present v_1 of protons in our calculation with parameters chosen to mock up a RHIC collision with 20-30% centrality for protons with $p_T = 0.5$, 1 and 2 GeV. As in Fig. 6, we see that the magnitude of the Faraday contribution to v_1 increases with increasing p_T. In Fig. 8 we see that the sign of v_1 flips as p_T increases, as the Faraday contribution goes from being smaller than to larger than the Hall contribution.

V. OBSERVABLES, AND A LOOK AHEAD

Our estimates of the magnitude of the charge-dependent directed flow of pions and (anti)protons in heavy ion collisions at the LHC and RHIC, and their dependence on Y and p_T, can be found in Figs. 4, 6, 7 and 8. If we focus on $Y \sim 1$ and $p_T \sim 1$ GeV, we see that the magnitude of the contribution to v_1 due to the magnetic field is between 10^{-5} and 10^{-4}, with the effect being about twice as large at in heavy ion collisions at top RHIC energies than in those at the LHC and about twice as large for pions than for (anti)protons. So, the effect is small. What makes it distinctive is that it is opposite in sign for positively and negatively charged particles of the same mass, and that for any species it is odd in rapidity.

Detecting the effect directly by measuring the directed flow of positively and negatively charged particles, which we shall denote by v_1^+ and v_1^-, is possible in principle but is likely to be prohibitively difficult in practice for two reasons. First, event-by-event there can be significant charge-independent contributions to v_1 due to event-by-event variation in the "shape" (in the transverse plane) of the energy deposited by the collision. This means that a separate measurement of v_1^+ and v_1^- followed by subtracting one measured quantity from the other would require enormous data sets and very precise control of each of the two separate measurements. Second, the separate measurement of either v_1^+ or v_1^- requires reconstructing the direction of the magnetic field in each event (i.e. determining event by event whether B_y is positive or negative) by using forward detectors to measure the directions in which the remnants of the colliding ions are deflected. It would be advantageous to define correlation observables that, first of all, involve taking ensemble averages of suitably chosen differences rather than just of v_1^+ or v_1^- and that, second of all, do not require knowledge of the direction of the magnetic field. The construction of such observables can be guided by symmetry considerations that apply in collisions between like nuclei that dictate that the contribution to the directed flow that is caused by the electric currents induced by a magnetic field created in the collision must satisfy

$$v_1^+(Y) = -v_1^-(Y) = -v_1^+(-Y) = v_1^-(-Y) \qquad (5.1)$$

for either pions or (anti)protons, for any value of p_T, and regardless of the direction of the magnetic field. Here $Y = 0$ means particles produced at $90°$ to the beam direction in the center-of-mass frame.

To isolate the charge-dependent directed flow that we are after, namely the effect of an electric current as in Fig. 1 that must satisfy (5.1) event-by-event, and to separate it from larger charge-independent effects it is helpful to define the following asymmetries between the directed flows for positive and negative hadrons:

$$\begin{aligned} A_1^{+-}(Y_1, Y_2) &\equiv v_1^+(Y_1) - v_1^-(Y_2), \\ A_1^{++}(Y_1, Y_2) &\equiv v_1^+(Y_1) - v_1^+(Y_2), \\ A_1^{--}(Y_1, Y_2) &\equiv v_1^-(Y_1) - v_1^-(Y_2), \end{aligned} \qquad (5.2)$$

and to measure correlations of these asymmetries. It is easy to see from (5.1) that for the effects induced by a magnetic field

$$\begin{aligned} A_1^{+-}(Y, Y) &= 2v_1^+(Y) = -A_1^{+-}(-Y, -Y) \\ &= A_1^{++}(Y, -Y) = A_1^{--}(-Y, Y), \end{aligned} \qquad (5.3)$$

and so on. Even if the direction of the magnetic field is not reconstructed, one can still study the correlation functions defined by

$$C_1^{i,j}(Y_1, Y_2) \equiv \langle A_1^i(Y_1, Y_2) A_1^j(Y_1, Y_2)\rangle. \qquad (5.4)$$

These correlation functions are quadratic in the directed flow, and so are not sensitive to the direction of $\vec{B}$ and the

sign of v_1 in a given event. However, they still carry the requisite information about dynamical charge-dependent correlations induced by the magnetic field. Analogous correlations functions have been measured with high precision [12, 13]. Using the relations (5.1) and (5.3), one can easily construct the desired correlators, and can then predict their signs and magnitudes using our results from Section IV. Let us list four examples. First, consider

$$\begin{aligned} C_1^{+-,+-}(Y, Y) &\equiv \langle A_1^{+-}(Y, Y) A_1^{+-}(Y, Y)\rangle \\ &= 4\langle v_1^+(Y) v_1^+(Y)\rangle, \end{aligned} \qquad (5.5)$$

where we have used (5.1) in the second equality. Charge-independent contributions to v_1 that do not satisfy (5.1) will cancel in (5.5). Second, in addition to measuring $C_1^{+-,+-}(Y, Y)$ with the goal of extracting $\langle v_1^+(Y) v_1^+(Y)\rangle$ it is very important at the same time to measure

$$\begin{aligned} C_1^{+-,+-}(Y, -Y) &\equiv \langle A_1^{+-}(Y, -Y) A_1^{+-}(Y, -Y)\rangle \\ &= 0, \end{aligned} \qquad (5.6)$$

since according to (5.1) this correlator should vanish, as indicated by the last equality. One can of course also measure

$$\langle (v_1^+(Y) + v_1^-(-Y))^2\rangle = 4\langle v_1^+(Y) v_1^+(Y)\rangle, \qquad (5.7)$$

where we have used (5.1) in the equality. Fourth, consider

$$\begin{aligned} C_1^{++,--}(Y, -Y) &\equiv \langle A_1^{++}(Y, -Y) A_1^{--}(Y, -Y)\rangle \\ &= 2\langle v_1^+(Y) v_1^-(Y) - v_1^+(Y) v_1^-(-Y)\rangle \\ &= -4\langle v_1^+(Y) v_1^+(Y)\rangle, \end{aligned} \qquad (5.8)$$

where we have used (5.1) in the last equality. So, to give an example of a possible analysis strategy, imagine measuring the four correlators (5.5), (5.6), (5.7) and (5.8) in heavy ion collisions at RHIC or the LHC, for pions or for (anti)protons or for that matter for charged hadrons. Contributions to these correlators arising from the electric current induced by the Hall and Faraday effects due to the presence of a magnetic field will vanish in (5.6), will be equal in (5.5) and (5.7), and will be equal in magnitude but opposite in sign in (5.8). Measuring correlations that fit this pattern will allow for the determination of $\langle v_1^+(Y) v_1^+(Y)\rangle$, which could then be compared to the results of calculations like those we have presented in Section IV.

Finally, it may also be advantageous to measure the components of (5.8), namely $\langle v_1^+(Y) v_1^-(Y)\rangle$ and $\langle v_1^+(Y) v_1^-(-Y)\rangle$, separately. Measuring each of these correlators and showing that they are both nonzero, are equal in magnitude, and that the first is negative while the second is positive would also constitute strong evidence for the charge-dependent and rapidity-odd contribution to the directed flow induced by the magnetic field present during the collision.

The challenge to experimentalists is to measure these correlators, or others that are also defined so as to separate the effects that satisfy (5.1) from charge-independent

backgrounds. If this is possible, one can imagine that it may be possible to use comparisons between data and the nontrivial p_T- and Y-dependence of results like those that we have obtained in Figs. 4, 6, 7 and 8 to extract a wealth of information, for example about the strength of the initial magnetic field and about the magnitude of the electrical conductivity of the plasma.

Before such goals can be realized, however, there remain many challenges on the theoretical side. We have made many simplifying assumptions, justifying them by virtue of the fact that our goal in this paper is only order-of-magnitude estimates of the Hall and Faraday effects on the charge-dependent directed flow. Given that the magnitude of the observable effect turns out to result from a partial cancellation between the Hall and Faraday effects, and given the interesting and quite nontrivial dependence of our results on Y and p_T, there is plenty of motivation for a more sophisticated, less simplified, treatment. In our view, the most pressing challenges are the inclusion of temperature-dependent, and therefore spacetime-dependent, electrical conductivity σ and drag parameter μm, as well as the *ab initio* calculation of the second of these two quantities. Treating both these quantities as temperature-dependent, rather than as constants, will require an analysis in which the solution of Maxwell's equations is done numerically, rather than analytically as in Section II. Once this threshold has been crossed, there will be no motivation to use Gubser's analytic solution to the hydrodynamic equations. At this point it will be best to use a state-of-the-art (3+1)-dimensional numerical relativistic viscous hydrodynamics calculation. Even further in the future it may become relevant to consider the back reaction of the effects induced by the magnetic field on the hydrodynamics itself. However, given the smallness of the effects that we have found, attempting this even more challenging extension of our analysis does not seem to be pressing.

A natural direction for further investigation is lower energy heavy ion collisions, as in the RHIC Beam Energy Scan program. Heavy ion collisions with $\sqrt{s}$ as low as 7.7 AGeV have been studied in the first, exploratory, phase of this program. The STAR collaboration has measured the directed flow v_1 for positively and negatively charged pions and for protons and antiprotons in these lower energy collisions [42]. These preliminary data show hints of the effects of magnetic fields that we have described, for example with v_1 for positively charged pions less than (greater than) v_1 for negatively charged pions with $Y > 0$ ($Y < 0$), as when the Faraday effect dominates over the Hall effect, in collisions with $\sqrt{s} = 7.7$ and 11.5 AGeV. This motivates the measurement of the directed flow correlations that we have proposed. High statistics data sets at these low collision energies are anticipated in a few years, after the implementation of a RHIC upgrade involving adding electron cooling for lower energy heavy ion beams.

Since we have found that the observable effects of magnetic fields on the charge-dependent directed flow are greater at top RHIC energies than at LHC energies, it is natural to expect that the effects will be greater still in lower energy collisions at RHIC. At these lower energies, however, the calculation of these effects is much more challenging for several reasons. The matter produced in the collision spends less time in the QGP phase meaning that it spends a larger fraction of its time in the vicinity of the crossover or transition between QGP and hadron gas, and in the hadron gas phase. This makes the use of a constant σ and the use of a solution to conformal hydrodynamics, like Gubser's, less viable even as qualitative guides. We look forward to estimating the magnitude of the directed flow correlators that we have introduced in this paper in lower energy collisions in the future, once a treatment with σ varying in space and time and with more realistic hydrodynamics is in hand. Also, at the lowest energies the assumption that we made in calculating the magnetic field that the spectators travel along straight lines will no longer be valid. Finally, the assumption that all the fragments of the incident nucleons (spectators and participants) end up at large $|Y|$, well separated from the smaller values of $|Y|$ where we look for effects of the magnetic field, must also break down in lower energy collisions with smaller beam rapidity. For all these reasons, further calculations are needed before firm conclusions can be drawn from the low energy data. And, there are strong motivations for measuring the directed flow correlators that we have defined in heavy ion collisions at top RHIC energy and at the LHC, where our estimates should be more reliable.

[1] D. E. Kharzeev, L. D. McLerran and H. J. Warringa, Nucl. Phys. A **803**, 227 (2008) [arXiv:0711.0950 [hep-ph]].

[2] V. Skokov, A. Y. Illarionov and V. Toneev, Int. J. Mod.

Phys. A **24**, 5925 (2009) [arXiv:0907.1396 [nucl-th]].

[3] K. Tuchin, Phys. Rev. C **82**, 034904 (2010) [Erratum-ibid. C **83**, 039903 (2011)] [arXiv:1006.3051 [nucl-th]].

[4] V. Voronyuk, V. D. Toneev, W. Cassing, E. L. Bratkovskaya, V. P. Konchakovski and S. A. Voloshin, Phys. Rev. C **83**, 054911 (2011) [arXiv:1103.4239 [nucl-th]].

[5] W. -T. Deng and X. -G. Huang, Phys. Rev. C **85**, 044907 (2012) [arXiv:1201.5108 [nucl-th]].

[6] K. Tuchin, Adv. High Energy Phys. **2013**, 490495 (2013) [arXiv:1301.0099].

[7] L. McLerran and V. Skokov, arXiv:1305.0774 [hep-ph].

[8] K. Fukushima, D. E. Kharzeev and H. J. Warringa, Phys. Rev. D **78**, 074033 (2008) [arXiv:0808.3382 [hep-ph]].

[9] D. E. Kharzeev and H.-U. Yee, Phys. Rev. D **83**, 085007 (2011) [arXiv:1012.6026 [hep-th]].

[10] Y. Burnier, D. E. Kharzeev, J. Liao and H.-U. Yee, Phys. Rev. Lett. **107**, 052303 (2011) [arXiv:1103.1307 [hep-ph]].

[11] G. Basar, D. Kharzeev, D. Kharzeev and V. Skokov, Phys. Rev. Lett. **109**, 202303 (2012) [arXiv:1206.1334 [hep-ph]].

[12] B. I. Abelev *et al.* [STAR Collaboration], Phys. Rev. Lett. **103**, 251601 (2009) [arXiv:0909.1739 [nucl-ex]].

[13] B. I. Abelev *et al.* [STAR Collaboration], Phys. Rev. C **81**, 054908 (2010) [arXiv:0909.1717 [nucl-ex]].

[14] B. Abelev *et al.* [ALICE Collaboration], Phys. Rev. Lett. **110**, 012301 (2013) [arXiv:1207.0900 [nucl-ex]].

[15] G. Wang [STAR Collaboration], Nucl. Phys. A904-905 **2013**, 248c (2013) [arXiv:1210.5498 [nucl-ex]].

[16] A. Drees [PHENIX Collaboration], Nucl. Phys. A **910-911**, 179 (2013).

[17] L. Adamczyk *et al.* [STAR Collaboration], arXiv:1302.3802 [nucl-ex].

[18] L. Adamczyk *et al.* [STAR Collaboration], arXiv:1303.0901 [nucl-ex].

[19] S. Schlichting and S. Pratt, Phys. Rev. C **83**, 014913 (2011) [arXiv:1009.4283 [nucl-th]].

[20] A. Bzdak, V. Koch and J. Liao, Lect. Notes Phys. **871**, 503 (2013) [arXiv:1207.7327].

[21] A. Bzdak and P. Bozek, Phys. Lett. B **726**, 239 (2013) [arXiv:1303.1138 [nucl-th]].

[22] H.-T. Ding, A. Francis, O. Kaczmarek, F. Karsch, E. Laermann and W. Soeldner, Phys. Rev. D **83**, 034504 (2011) [arXiv:1012.4963 [hep-lat]].

[23] A. Francis and O. Kaczmarek, Prog. Part. Nucl. Phys. **67**, 212 (2012) [arXiv:1112.4802 [hep-lat]].

[24] B. B. Brandt, A. Francis, H. B. Meyer and H. Wittig, JHEP **1303**, 100 (2013) [arXiv:1212.4200 [hep-lat]].

[25] A. Amato, G. Aarts, C. Allton, P. Giudice, S. Hands and J. -I. Skullerud, Phys. Rev. Lett. **111**, 172001 (2013) [arXiv:1307.6763 [hep-lat]].

[26] O. Kaczmarek and M. Mller, arXiv:1312.5609 [hep-lat].

[27] S. S. Gubser, Phys. Rev. D **82**, 085027 (2010) [arXiv:1006.0006 [hep-th]].

[28] D. Kharzeev and M. Nardi, Phys. Lett. B **507**, 121 (2001) [nucl-th/0012025].

[29] D. Kharzeev, E. Levin and M. Nardi, Nucl. Phys. A **747**, 609 (2005) [hep-ph/0408050].

[30] F. Cooper and G. Frye, Phys. Rev. D **10**, 186 (1974).

[31] C. P. Herzog, A. Karch, P. Kovtun, C. Kozcaz and L. G. Yaffe, JHEP **0607**, 013 (2006) [hep-th/0605158].

[32] J. Casalderrey-Solana and D. Teaney, Phys. Rev. D **74**, 085012 (2006) [hep-ph/0605199].

[33] S. S. Gubser, Phys. Rev. D **74**, 126005 (2006) [hep-th/0605182].

[34] D. Kharzeev, Phys. Lett. B **378**, 238 (1996) [nucl-th/9602027].

[35] E. Abbas *et al.* [ALICE Collaboration], Eur. Phys. J. C **73**, 2496 (2013) [arXiv:1305.1562 [nucl-ex]].

[36] S. Borsanyi, G. Endrodi, Z. Fodor, A. Jakovac, S. D. Katz, S. Krieg, C. Ratti and K. K. Szabo, JHEP **1011**, 077 (2010) [arXiv:1007.2580 [hep-lat]].

[37] H. B. Meyer, Phys. Rev. D **76**, 101701 (2007) [arXiv:0704.1801 [hep-lat]].

[38] C. Shen and U. Heinz, Phys. Rev. C **85**, 054902 (2012) [Erratum-ibid. C **86**, 049903 (2012)] [arXiv:1202.6620 [nucl-th]].

[39] B. Abelev *et al.* [ALICE Collaboration], Phys. Rev. C **88**, 044910 (2013) [arXiv:1303.0737 [hep-ex]].

[40] S. S. Adler *et al.* [PHENIX Collaboration], Phys. Rev. C **69**, 034909 (2004) [nucl-ex/0307022].

[41] A. Rybicki and A. Szczurek, Phys. Rev. C **87**, 054909 (2013) [arXiv:1303.7354 [nucl-th]].

[42] Y. Pandit [STAR Collaboration], Acta Phys. Polon. Supp. **5**, 439 (2012) [arXiv:1112.0842 [nucl-ex]].